



Response of the MIMOSA-28 pixel sensor to a wide range of ion species and energies

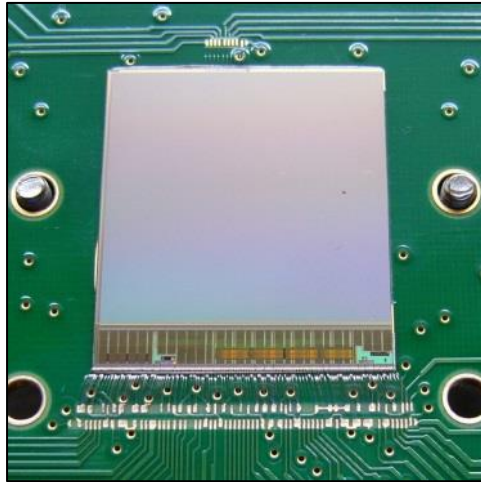
Claire-Anne Reidel
GSI Biophysics department
c.a.reidel@gsi.de

Motivations

- Monolithic Active Pixel Sensors (MAPS) are used as vertex detector
 - High energy physics
 - Particle therapy and Space radiation applications
- Characterization of the MIMOSA-28 pixel sensor cluster size (number of fired pixels) as a function of the energy deposition
 - Several species: protons, helium, carbon, argon and iron ions
 - Energy loss: 10–14000 keV
 - Semi-empirical model development: based on diffusion and Coulomb expansion
- Particle identification with MIMOSA-28?

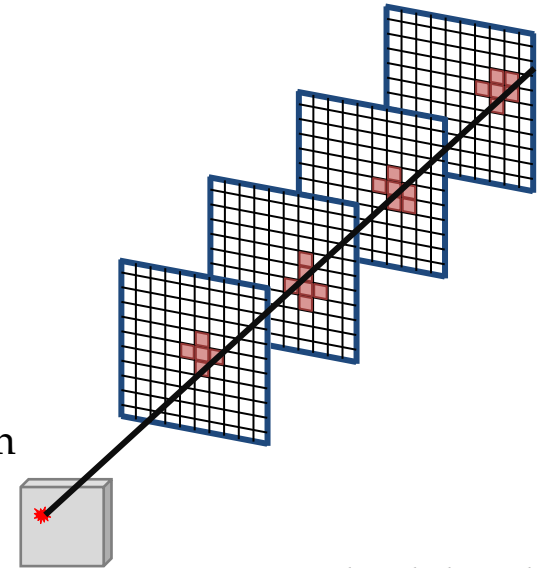
MIMOSA-28 sensor

Measurements of charged particle trajectories with high resolution



*Developed by PICSEL group,
IPHC Strasbourg*

- CMOS technology
- Active area: $\sim 2 \times 2 \text{ cm}^2$
- Pixel size: $20.7 \mu\text{m}$
- Epitaxial layer: $14 \mu\text{m}$
- Readout time: $186.5 \mu\text{s}$
- Spatial resolution: $\sigma < 10 \mu\text{m}$
- Binary output

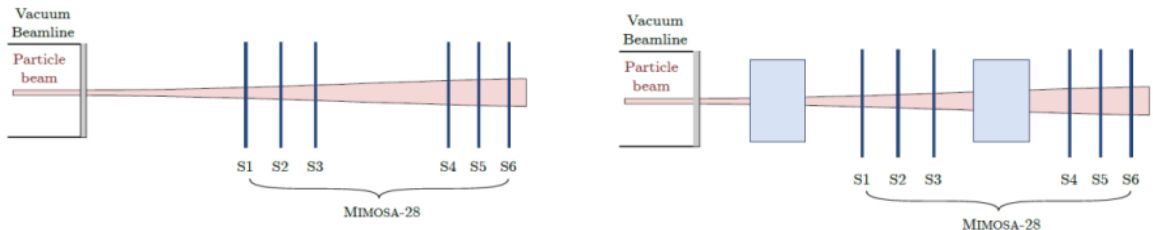


Reconstructed track through the
different clusters and vertex

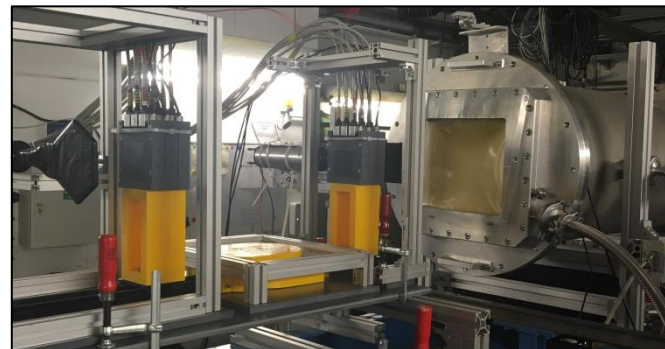
Experimental campaign

Beamtime campaign

- Several accelerator facilities:
 - GSI Helmholtzzentrum für Schwerionenforschung GmbH (SIS10 & UNILAC)
 - Heidelberg and Marburg ion-beam therapy centers
- Example of experimental setup configurations with six MIMOSA-28 pixel sensors:



Experimental setup with six Mimosas-28 placed along the beam axis without any target (left) and with a target placed in front and in-between two sets of three sensors (right)



*GSI Helmholtzzentrum für Schwerionenforschung,
@ Cave A*



Marburg ion-beam therapy center

Experimental campaign

Particle beams

| Particle | E_0 (MeV/u) | Setup | E_1 (MeV/u) | ΔE (keV) | |
|-----------------------------|-----------------------------|-------------------|---------------|-----------------------|--------------------|
| $^1\text{H}^{1+}$ ions | 150.14 ^a | (a)-S1 | 148.8 | 14.3 (-0.1,+0.1) | |
| | 150.14 ^a | (b)-S4 | 124.3 | 16.2 (-0.1,+0.1) | |
| $^4\text{He}^{2+}$ ions | 3.6 ^c | (a)-S1 | 2.9 | 1156.2 (-22,+23) | |
| | 3.6 ^c | (c)-S1 | 2.2 | 1427.0 (-82,+101) | |
| | 3.6 ^c | (a)-S2 | 1.0 | 2375.0 (-431,+1180) | |
| | 80.64 ^b | (a)-S1 | 78.2 | 90.7 (-0.2,+0.2) | |
| | 130.25 ^b | (a)-S1 | 128.6 | 63.2 (-0.1,+0.1) | |
| | 220.51 ^b | (a)-S1 | 219.3 | 44.4 (-0.1,+0.1) | |
| | 11.4 ^c | (a)-S1 | 10.6 | 3942.3 (-24,+24) | |
| | 11.4 ^c | (a)-S2 | 9.0 | 4456.0 (-82,+88) | |
| $^{12}\text{C}^{6+}$ ions | 11.4 ^c | (a)-S3 | 7.1 | 5277.9 (-219,+254) | |
| | 11.4 ^c | (c)-S1 | 5.1 | 6595.4 (-237,+268) | |
| | 11.4 ^c | (c)-S2 | 1.5 | 12554.2 (-2401,+4692) | |
| | 180 ^d | (a)-S1 | 171.1 | 469.6 (-0.5,+1.9) | |
| | 278.84 ^a | (a)-S1 | 270.3 | 354.4 (-0.6,+0.6) | |
| | 278.84 ^a | (d)-S1 | 152.4 | 507.3 (-6.1,+6.5) | |
| | 278.84 ^a | (d)-S4 | 69.3 | 896.4 (-69,+94) | |
| | 287.50 ^a | (a)-S1 | 284.9 | 344.0 (-0.2,+0.2) | |
| | 287.50 ^a | (b)-S4 | 238.2 | 381.5 (-1.5,+1.5) | |
| | 294.97 ^a | (a)-S1 | 286.7 | 342.8 (-0.5,+0.5) | |
| | 294.97 ^a | (d)-S1 | 175.3 | 462.2 (-4.3,+4.5) | |
| | 294.97 ^a | (d)-S4 | 105.3 | 657.0 (-25,+29) | |
| $^{40}\text{Ar}^{18+}$ ions | 310.61 ^a | (a)-S1 | 302.6 | 332.8 (-0.5,+0.5) | |
| | 310.61 ^a | (d)-S1 | 196.3 | 429.7 (-3.2,+3.3) | |
| | 310.61 ^a | (d)-S4 | 133.8 | 554.2 (-14,+15) | |
| | 225 ^d | (a)-S1 | 223.6 | 3596.7 (-2.1,+2.1) | |
| | $^{56}\text{Fe}^{25+}$ ions | 1000 ^d | (a)-S1 | 995.6 | 4084.2 (-0.2,+0.2) |

➤ Particle species:

- Protons
- ^4He ions
- ^{12}C ions
- ^{40}Ar ions
- ^{56}Fe ions

➤ Particle energies:

- From 10 MeV/u up to 1 GeV/u

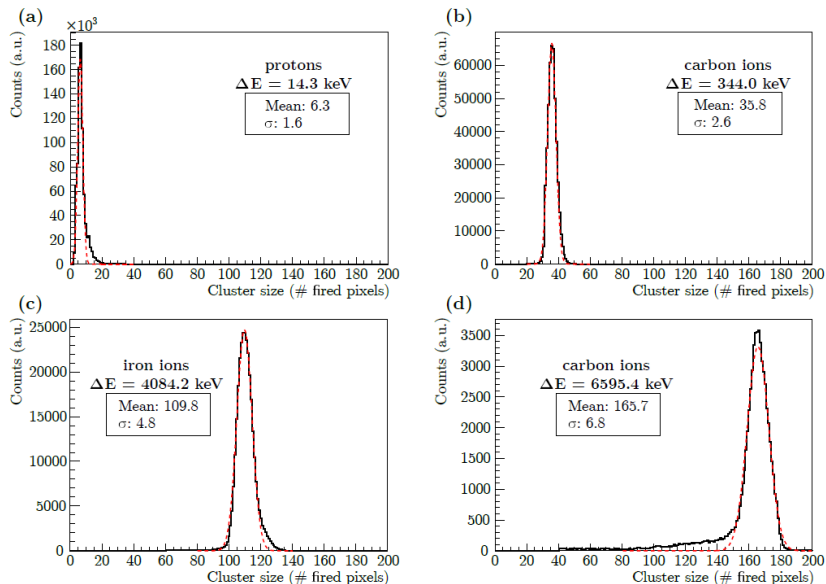
➤ Energy loss in 14 μm silicon:

- From 10 up to 14000 keV

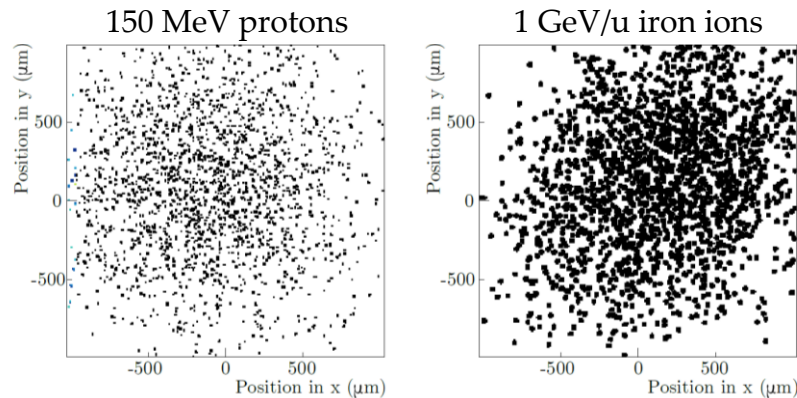


Cluster size distributions

Cluster size distributions to different particles and energies



Cluster maps of MIMOSA-28

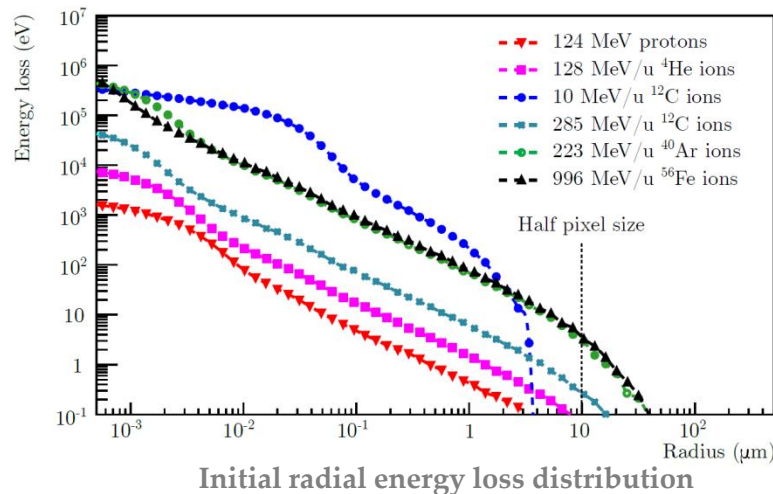


- Dependence on the energy loss
- Dependence on particle species?

C.-A. Reidel et al., NIMA, 2021

Initial radial distributions

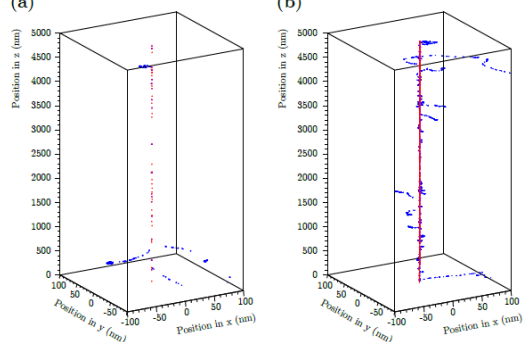
Track structure & Radial energy distributions



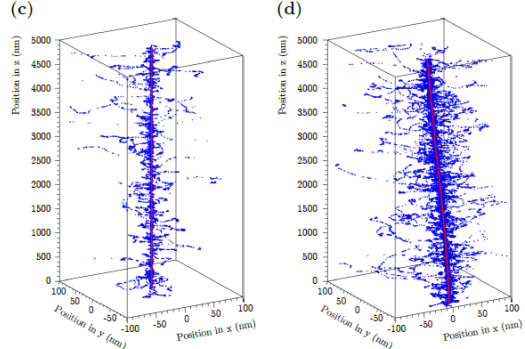
- Dependence on the particle species and energy
- Initial radial energy loss distribution smaller than one pixel for MIMOSA-28

C.-A. Reidel et al., NIMA, 2021

150 MeV protons (a) 285 MeV/u ^{12}C (b)



1 GeV/u ^{56}Fe (c) 5 MeV/u ^{12}C (d)



Ion track structure passing through 5 μm silicon layer

Semi-empirical model

Cluster size as a function of the energy loss

- Spatial charge density is described by a Gaussian as a function of the radius:

$$\frac{dq(r)}{dA} = \frac{Q_{tot}}{2\pi\sigma_{tot}^2} \exp\left(-\frac{r^2}{2\sigma_{tot}^2}\right)$$

- Based on diffusion and Coulomb expansion:

$$\sigma_{tot}^2 = \underbrace{(w_D\sigma_D)^2}_{\text{Diffusion}} + \underbrace{(w_C\sigma_C)^2}_{\text{Coulomb expansion}}$$

- Energy loss dependence from the Coulomb expansion component:

$$\sigma_{tot} = \sqrt{w_D^2 2Dt + w_C^2 \left(\frac{3\mu_e Q_{tot} t}{4\pi\epsilon_0\epsilon_r}\right)^{2/3}}, \quad Q_{tot} = e\Delta E/E_i$$

➤ Number of fired pixels:

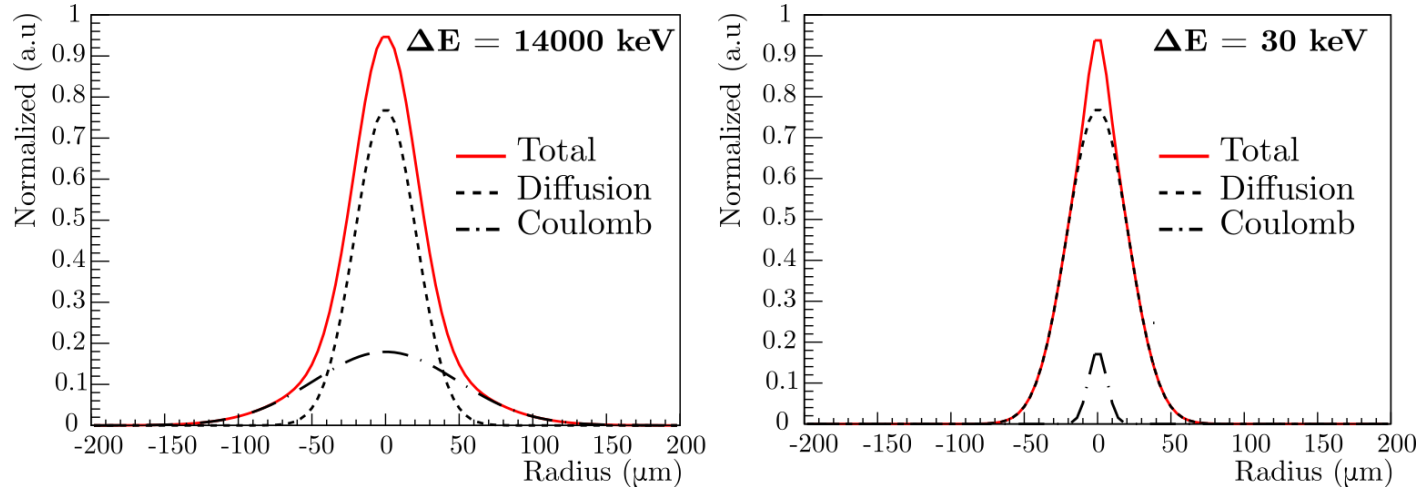
$$n_p = \frac{2\pi\sigma_{tot}^2}{p^2} \ln\left(\frac{e\Delta E/E_i}{2\pi\sigma_{tot}^2 n Q_n/p^2}\right)$$

➤ Three free parameters:

- w_D : scaling diffusion factor
- w_C : scaling Coulomb expansion factor
- Q_n : intrinsic noise charges

Semi-empirical model

Diffusion and Coulomb expansion contributions

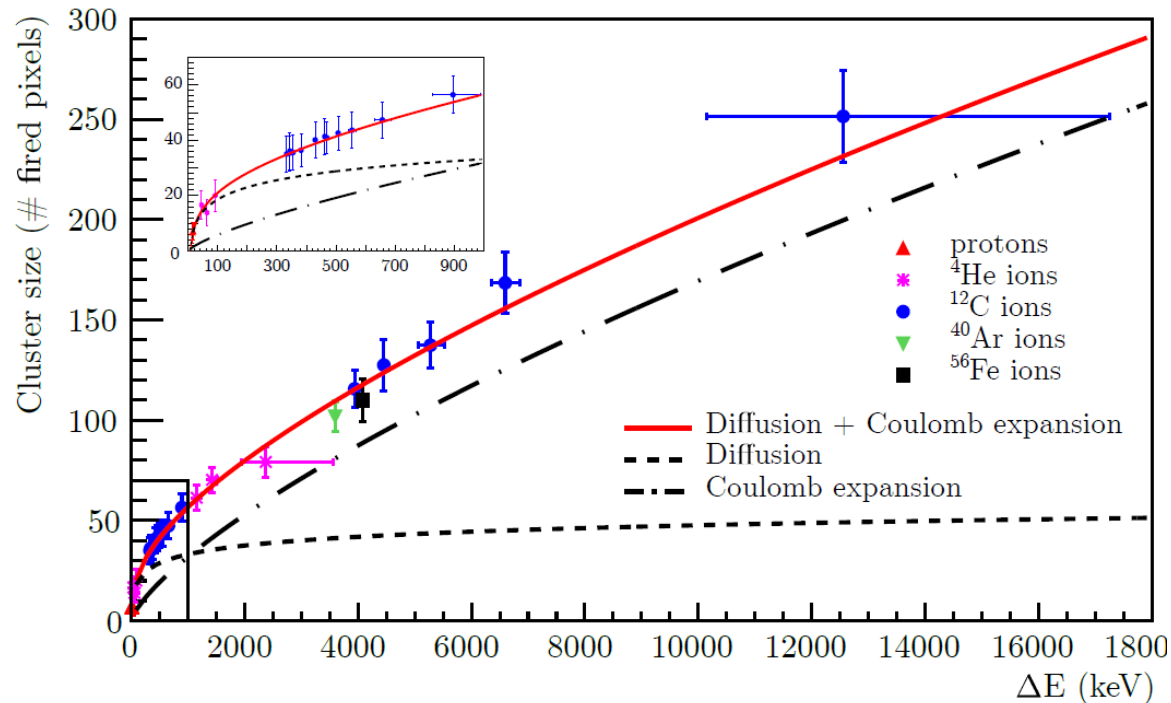


Electron cloud propagation as a function of the radius

- Coulomb expansion becomes significant for high energy losses (dense ion tracks) and contributes to the Gaussian tail

C.-A. Reidel et al., NIMA, 2021

MIMOSA-28 sensor response

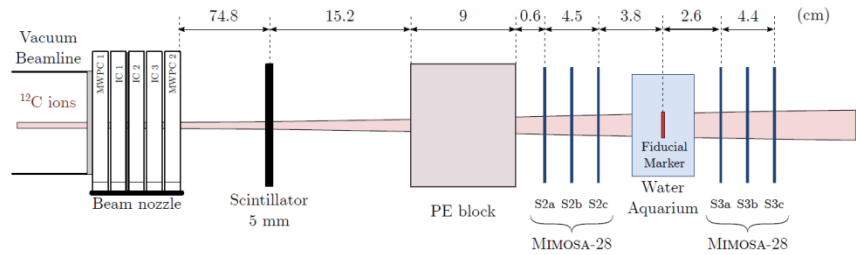


Cluster size vs. ΔE

- Diffusion dominates for $\Delta E < 1000$ keV
- Coulomb expansion (energy loss dependent) dominates for $\Delta E > 1000$ keV
- Optimized free parameters:
 - $w_D = 0.81 \pm 0.08$
 - $w_C = 0.19 \pm 0.008$
 - $Q_n = 38 \pm 13 e^-$

Particle identification with MIMOSA-28?

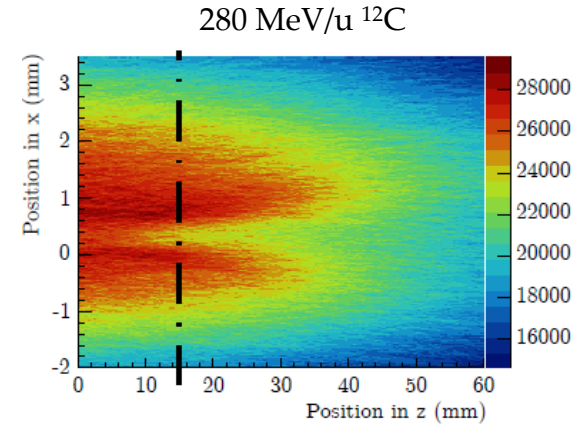
Experimental study for fluence perturbations due to fiducial markers used in ion-beam therapy



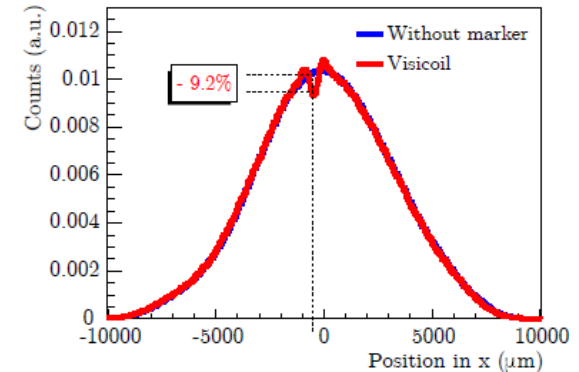
Fiducial marker

Visicoil

$\varnothing = 0.5$ mm
 $L = 10$ mm
 $m = 24$ mg

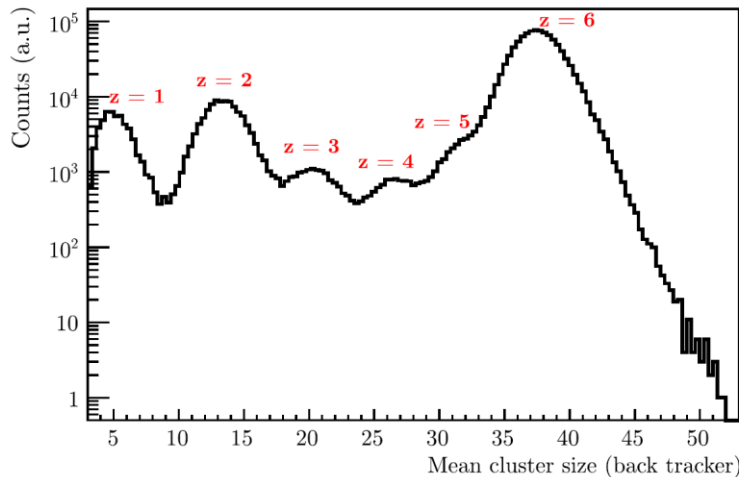


- Three dimensional fluence distribution from all reconstructed tracks
- Quantification of the fluence perturbation due to fiducial markers for particle therapy
- Possibility of particle identification additionally to the particle trajectory for improved analysis?



Particle identification with MIMOSA-28?

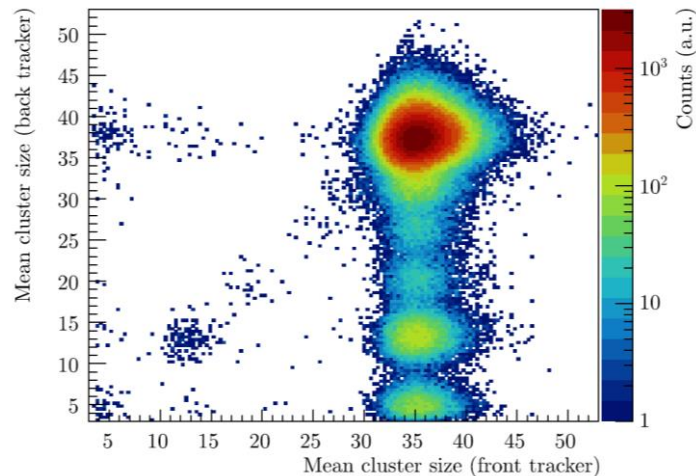
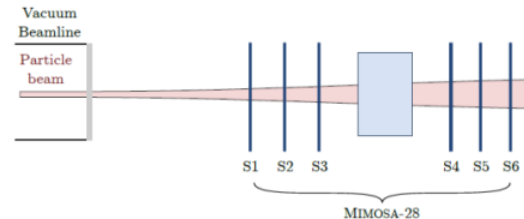
Response to a complex field



Mean cluster size of the clusters belonging to a track

- Mean cluster size dependence Z
- Primary ion separation
- Additional tool for larger experiments

285 MeV/u ¹²C impinging on 4 cm water target



Published in C.-A. Reidel, NIMA, 2021

Conclusions & Outlook

- Long row of accelerator experiments for the characterization of the MIMOSA-28 response
 - Protons to iron ions in the energy range 10 MeV/u – 1 GeV/u
- Cluster size distribution study
- Semi-empirical model development based on diffusion and Coulomb expansion phenomena
 - Describes the cluster size as a function of the energy loss
 - Optimization of three free parameters of the model
- MIMOSA-28 can be used as an additional tool for particle identification
- Development of MAPs with analog output for particle identification and tracking

Acknowledgements

➤ GSI Biophysics, Darmstadt

- Christoph Schuy
- Felix Horst
- Daria Boscolo
- Thomas Friedrich
- Marco Durante
- Uli Weber



➤ IPHC, Strasbourg

- Christian Finck
- Marie Vanstalle
- Jérôme Baudot

